

# SYNTHETIC APERTURE RF RECEPTION USING RYDBERG ATOMS

Nikunj Kumar Prajapati<sup>1</sup>, Alexandra Artusio-Glimpse<sup>1</sup>, Matthew Simons<sup>1</sup>, Samuel Berweger<sup>1</sup>,  
Andrew Rotunno<sup>1</sup>, Maitreyi Jayaseelan<sup>2</sup>, Kaleb Campbell<sup>2</sup>, Christopher Holloway<sup>1</sup>

<sup>1</sup>National Institute of Standards and Technology, Boulder, CO 80305, USA

<sup>2</sup>University of Colorado, Boulder, CO 80305, USA

## ABSTRACT

Rydberg atoms show great promise for use as self-calibrated electric field sensors for a broad range of frequencies. Their response is traceable to the international system of units making them a valuable tool for a variety of applications including traceable channel sounding. The Rydberg atom sensor is an electrically small point probe. Its detection volume is defined by the overlap of probing and coupling lasers, which can be as small as hundreds of microns. We present measurements of the beam-formed output of a horn antenna in the far field at 28 GHz. We move a Rydberg atom sensor over a synthetic aperture to obtain high angular resolution of the received signal and employ electromagnetically induced transparency with AC Stark shifting and a local oscillator signal radiated onto the atoms for magnitude and phase detection at each location in the area. These results demonstrate the use of these Rydberg atom sensors in a synthetic aperture configuration and inform their eventual use for traceable channel sounding measurements.

**Index Terms**— Rydberg atom, electric field sensor, aperture, quantum optics, electromagnetically induced transparency, Stark shift.

## 1. INTRODUCTION

Channel sounding is a technique that evaluates an environment for wireless communication and is often used to engineer solutions that allow for multi-band carriers to be transmitted and received in a space [1]. This requires the characterization of the radio environment to eliminate the effects of multiple paths that can interfere and overshadow the intended signal. Typically, a vector probe is moved around in an environment to produce a map of the environment that can be used to overcome or leverage complex multi-path trajectories. However, classical probes have certain limitations that can impede these measurements. Metallic antennas scatter incident waves and affect the measurement of the environment. In addition to this, to characterize the background noise environment accurately, the probe must be calibrated with traceability to a national metrology institute.

NIST-on-a-Chip IMS.

To avoid these issues, we utilize Rydberg atoms (highly excited atoms) as electric field probes. Rydberg atoms have a strong response to external fields, are SI-traceable to Planck's constant, and are nondispersive to radio frequency (RF) fields [2, 3, 4]. Rydberg atoms garnered substantial attention over the past decade where they have been used as RF power meters [5], spectrum analyzers [6], and receivers among others [7, 8, 9, 10]. By exposing the atoms to a local oscillator (LO) along with the RF signal, the Rydberg atoms act as a mixer and can be used to receive phase and amplitude modulated signals [9, 10]. This also allows for the determination of angle-of-arrival [11]. The Rydberg atom sensor can have a small form factor to be used as a low invasiveness sensor [12].

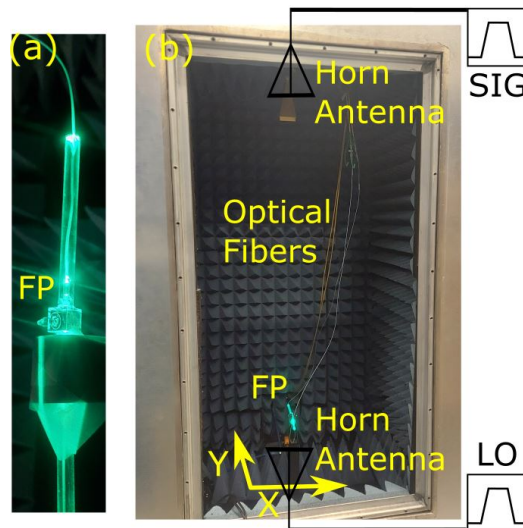


**Fig. 1.** (a) Fiber probe (FP). The two lasers are fed into the vapor cell via fiber and probe laser is readout via fiber. Cell is made of borosilicate glass. (b) Anechoic chamber with RF absorber placed throughout the inside of the chamber.

In this manuscript, we present measurements that utilize the Rydberg atoms in a synthetic aperture (SA) configuration to simulate a 2D array based receiver and perform high resolution imaging of a transmitter with a minimally perturbative receiver. We utilize electromagnetically induced transparency

(EIT) to establish and probe the Rydberg atoms [4]. We constructed a small fiber-coupled probe and placed it in an anechoic chamber to test the SA Rydberg receiver in a controlled environment. We placed the 10 mm x 10 mm Rydberg atom vapor cell filled with cesium atoms inside of the test chamber. The fiber probe mounted on a acetal resin stand that is supported on a 2-axis motorized stage controlled via USB. The stage has a movement range of 100 mm. We measure the electric field amplitude and phase as the probe is translated on a motorized stage, as shown in Fig 1 (a) and (b).

## 2. RYDBERG ATOMS AS FIELD SENSORS

Rydberg atom-based electric field sensors rely on exciting atoms to highly excited states in the energy manifold. These states exhibit a large atomic polarizability and therefore are very sensitive to external electric fields [3]. By monitoring the response of the atoms, we can accurately determine the electric field.

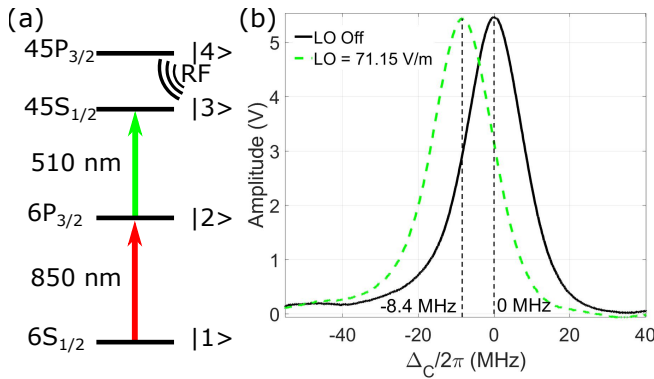


**Fig. 2.** (a) Level diagram of Cesium atom showing the ground state  $|1\rangle$ , intermediate state  $|2\rangle$ , and two Rydberg state  $|3\rangle$  and  $|4\rangle$ . (red) Probe laser used for readout. (blue) coupling laser to generate EIT and populate Rydberg state. (b) Sample transmission spectra. (black) Probe transmission spectra with no RF field applied. (red) Transmission spectra with off-resonant RF field applied. (green) Transmission spectra with off resonant RF field applied.

The Rydberg atoms are established and probed through a two-photon interaction known as electromagnetically induced transparency (EIT), shown by Fig. 2 (a). This allows for a narrow line spectroscopic measurement of the Rydberg state, shown by the black trace in Fig. 2 (b). In the presence of an RF field resonant from the Rydberg state ( $|1\rangle$ ) and an adjacent Rydberg state ( $|1\rangle$ ), the atomic state will split according to the Autler-Townes effect [4],

$$\Delta_f = \frac{|E|\wp}{\hbar}, \quad (1)$$

where  $E$  is the electric field,  $\hbar$  is the reduced Planck constant, and  $\wp$  is the transition dipole moment between the adjacent

Rydberg states. The transition dipole moment can be calculated to the 1% level and Planck's constant is a fundamental constant defined by the SI. By measuring the observed splitting, we can obtain a calibrated measurement of the resonant electric field.

The resonant frequencies for adjacent Rydberg states can span from less than 1 gigahertz to several terahertz by simply tuning to a state with a different principle quantum number  $n$ . Other methods also exist to tune to DC [13] and several MHz [14]. These rely on the AC-stark effect, an off resonant shift in the Rydberg energy level, shown by the green trace in Fig. 2 (b). The off resonant shift is given by [3],

$$\Delta_f = -\frac{\alpha|E|^2}{2\hbar}, \quad (2)$$

where  $\alpha$  is the polarizability of the state, which also can be accurately calculated. It should be noted from this equation that the response is steady state, meaning that the signal is automatically demodulated from the carrier into the base-band.

## 3. EXPERIMENTAL IMPLEMENTATION

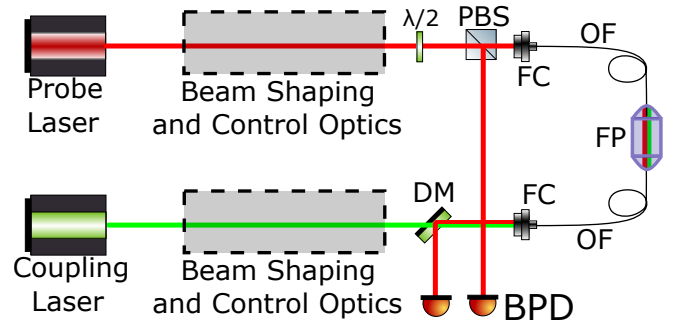


**Fig. 3.** Schematic of experiment. Abbreviations in text.

The experimental apparatus is shown in Fig. 3. We use an external cavity diode laser (ECDL) to generate the 850 nm probe laser light (red). The coupling laser beam (green) is derived from a 1020 nm ECDL that is amplified by a tapered amplifier and then doubled through a second harmonic generation cavity. Both lasers are passed through acousto-optic modulators (not shown) for power control and stabilization and then through beam shaping optics (not shown) for optimal fiber coupling.

The probe beam polarization is controlled using a  $\Lambda/2$  wave plate. Following the waveplate, the probe is split by a polarizing beam splitter (PBS) into a signal and a reference beam that is directly sent to one port of the balanced photodiode (BPD). The signal portion of the probe is then injected into the fiber coupler (FC) to send into the FP via the optical fiber (OF). The coupling laser is fiber coupled directly into the fiber probe without a reference pickoff.

Light from the probe and coupling lasers is collimated by gradient index lenses and arranged into a counter propagating

co-linear configuration through the vapor cell. Each ferrule is followed by a GRIN lens to size and shape the respective optical beams. The lenses are set so that the coupling beam is larger than the probe beam and to have optimal coupling of the probe beam into the coupling fiber for readout of the probe transmission. The probe signal is then output from the coupling laser FC. It is separated from the coupling laser using a dichroic mirror (DM) and then measured on the second port of the BPD. Once we achieved an EIT signal in the cell, all components making up the FP are set into place using a UV cured epoxy.

In this implementation, we utilize the off-resonant Stark effect to measure the beamformed output pattern of RF fields ranging in frequency from 28 GHz to 28.7 GHz. We tune our probe laser to be resonant with the  $6S_{1/2} - >6P_{3/2}$  transition in Cesium and the coupling laser to be resonant with the  $6P_{3/2} - >45S_{1/2}$  transition. The transition frequency between the Rydberg states  $45S_{1/2} - >45P_{3/2}$  is roughly 45 GHz; thus, 28 GHz is far from resonance and Eq. 2 applies. This far off-resonant state is selected to maintain the same polarizability across the entire Ka band (26.5 to 40 GHz). The presented measurements at 28 GHz are a proof-of-concept demonstration of these Rydberg atom measurements. Measurements across the entire Ka band are currently in process.

Fig. 2 (b) shows how the probe transmission signal changes with different applied powers to the horn antenna. By measuring the frequency shift from this stark effect, we can determine the electric field strength using Eq. 2. We also looked at the phase of the field by applying our own LO with an additional horn that translates with the Rydberg atom probe over the SA, shown in Fig. 1 (b). While this will produce additional reflections, we will later implement other methods that allow for phase measurement without a LO [15]. Since the response of the atoms given in Eq. 2 is based on the absolute value of the field, the atoms act as a mixer of the two RF fields [16, 17]. We apply an LO field that is shifted by 14 kHz from the signal field. This causes the green peak in Fig. 2 (b) to oscillate at the 14 kHz beatnote. We can retrieve the phase by measuring this beatnote through lockin detection.

#### 4. RESULTS AND DISCUSSION

We complete phase measurements of the signal field. The measurements are repeated as we move the fiber probe over a SA defined by 35x35 measurements spaced by 3.75 mm in a plane perpendicular to the line of sight of a horn antenna at the ceiling of the chamber. The fiber probe is mounted on a acetal resin stand that is supported on a 2-axis motorized stage controlled via USB. The stage has a maximum movement range of 100 mm along both axes. We lock the laser to the side of the atomic resonance and record the magnitude and phase output of a lock-in amplifier. The magnitude is flat across the translation profile, so we present the phase of the beat-note as a function of spatial location in Fig. 4. The phase map matches the expected phase for a horn antenna output

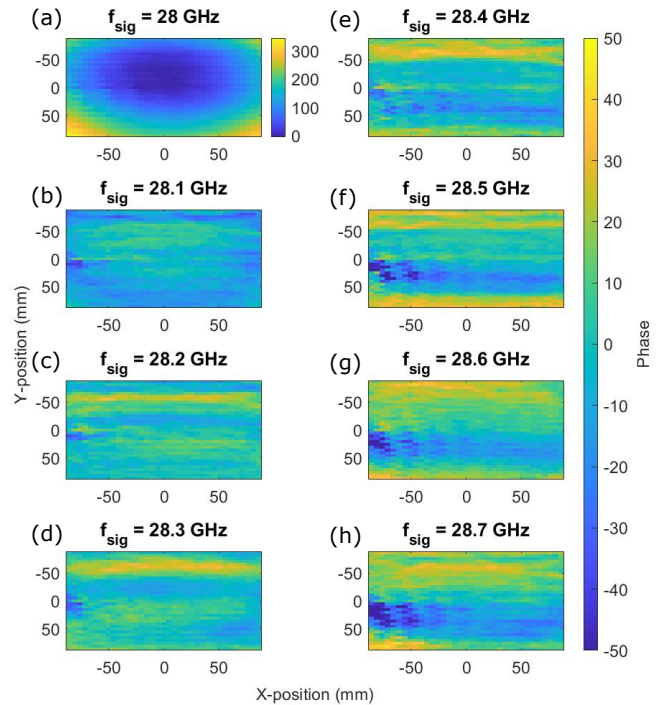


**Fig. 4.** (a) Phase measurement by Rydberg probe as the probe is translated across the chamber along the x and y axis for 28 GHz RF. (b-h) The phase difference from 28 GHz phase map for frequencies of the carrier wave, as labeled.

that is close to far field. As we tune the frequency of the signal, we can see how small differences in response based on frequency change the scattering in the reverberation chamber. To further demonstrate, we will look to introduce scattering elements in the chamber and map out the phase dependence in the chamber under more complex scattering conditions. We believe that this is a good first demonstration of the operation of the Rydberg atom probe as a synthetic aperture.

The Rydberg atom probe is electrically small compared to conventional antennas. For the 28 GHz field (10 mm wave), we are measuring in steps of 3.75 mm. However, the volume of measurement is considerably smaller than the step size since it is controlled by the size of the lasers. In this case, the lasers were roughly 100  $\mu\text{m}$ . With a different motor, we could map out the field with a much better resolution. Additionally, while the length of the cell or interaction is roughly 10 mm, other fields in the single digit gigahertz can also be mapped out with the same cell, allowing for sub-wavelength measurements.

In addition to making a Rydberg atom fiber probe to use as a synthetic aperture, we are also fabricating a photonic chip cell that can probe the atoms in a 2-d array [18, 19]. The photonic chip will allow for the measurement higher bandwidth signals due to the small interaction volumes with the atoms [20] and potentially lead to a stronger signal since we can pre-

form matched filtering for enhancement. In addition to this, the array will allow for application of new interesting phase estimation methods without a local oscillator [21].

## 5. CONCLUSION

We have demonstrated the capability of the Rydberg atom receiver as a synthetic aperture. By fabricating a fiber probe and making a chamber with minimal RF wave reflection, we were able to demonstrate the far field characteristics of a horn antenna. While this demonstration is the simplest base case, it gives credence to the Rydberg atom electric field sensor as a field probe. Furthermore, the use of the atoms allows for self-calibrated and low invasiveness measurements. The atom probe also allows for characterization of a large range frequencies by simply tuning the coupling laser to different atomic resonances. We have demonstrated the use of Rydberg atom probes as a new type of synthetic aperture for use in channel sounding.

## 6. COPYRIGHT

Publication of the U.S. government, not subject to U.S. copyright.

## 7. REFERENCES

- [1] Dave Laurenson and Peter Grant, "A review of radio channel sounding techniques," in *2006 14th European Signal Processing Conference*, 2006, pp. 1–5.
- [2] Alexandra Artusio-Glimpse, Matthew T. Simons, Nikunj Kumar Prajapati, and Christopher L. Holloway, "Modern RF Measurements With Hot Atoms: A Technology Review of Rydberg Atom-Based Radio Frequency Field Sensors," *IEEE Microwave Magazine*, vol. 23, no. 5, pp. 44–56, 2022.
- [3] Thomas F. Gallagher, *Rydberg Atoms*, Cambridge Monographs on Atomic, Molecular and Chemical Physics. Cambridge University Press, 1994.
- [4] Jonathon A. Sedlacek, Arne Schwettmann, Harald Kübler, Robert Löw, Tilman Pfau, and James P. Shaffer, "Microwave electrometry with Rydberg atoms in a vapour cell using bright atomic resonances," *Nature Physics*, vol. 9, no. 10, pp. 819–824, 2012.
- [5] Christopher L. Holloway, Matthew T. Simons, Marcus D. Kautz, Abdulaziz H. Haddab, Joshua A. Gordon, and Thomas P. Crowley, "A quantum-based power standard: Using Rydberg atoms for a SI-traceable radio-frequency power measurement technique in rectangular waveguides," *Applied Physics Letters*, vol. 113, no. 9, pp. 094101, 2018.
- [6] David H. Meyer, Paul D. Kunz, and Kevin C. Cox, "Waveguide-Coupled Rydberg Spectrum Analyzer from 0 to 20 GHz," *Phys. Rev. Applied*, vol. 15, pp. 014053, Jan 2021.
- [7] David Alexander Anderson, Rachel Elizabeth Sapiro, and Georg Raithel, "An Atomic Receiver for AM and FM Radio Communication," *IEEE Transactions on Antennas and Propagation*, vol. 69, no. 5, pp. 2455–2462, 2021.
- [8] J. Susanne Otto, Marisol K. Hunter, Niels Kjærgaard, and Amita B. Deb, "Data capacity scaling of a distributed Rydberg atomic receiver array," *Journal of Applied Physics*, vol. 129, no. 15, pp. 154503, 2021.
- [9] Zhenfei Song, Hongping Liu, Xiaochi Liu, Wanfeng Zhang, Haiyang Zou, Jie Zhang, and Jifeng Qu, "Rydberg-atom-based digital communication using a continuously tunable radio-frequency carrier," *Opt. Express*, vol. 27, no. 6, pp. 8848–8857, Mar 2019.
- [10] David H. Meyer, Kevin C. Cox, Fredrik K. Fatemi, and Paul D. Kunz, "Digital communication with Rydberg atoms and amplitude-modulated microwave fields," *Applied Physics Letters*, vol. 112, no. 21, pp. 211108, 2018.
- [11] A.K. Robinson, N. Prajapati, D. Senic, M.T. Simons, and C.L. Holloway, "Determining the angle-of-arrival of a radio-frequency source with a Rydberg atom-based sensor," *Applied Physics Letters*, vol. 118, pp. 114001, 2021.
- [12] Matt T. Simons, Joshua A. Gordon, and Christopher L. Holloway, "Fiber-coupled vapor cell for a portable Rydberg atom-based radio frequency electric field sensor," *Appl. Opt.*, vol. 57, no. 22, pp. 6456–6460, Aug 2018.
- [13] Christopher L. Holloway, Nikunj Kumar Prajapati, Jeffery A. Sherman, Alain Rüfenacht, Alexandra B. Artusio-Glimpse, Matthew T. Simons, Amy K. Robinson, David S. La Mantia, and Eric B. Norrgard, "Electromagnetically induced transparency based Rydberg-atom sensor for traceable voltage measurements, journal = AVS Quantum Science," vol. 4, no. 3, pp. 034401, 2022.
- [14] Andrew P. Rotunno, Samuel Berweger, Nikunj Kumar Prajapati, Matthew T. Simons, Alexandra B. Artusio-Glimpse, Christopher L. Holloway, Robert M. Potvliege, and C. S. Adams, "Pseudo-resonant Detection of 'Low Frequency' VHF Electric Fields via Rabi Matching with Autler-Townes Splitting in Rydberg Atoms," *arXiv*, 2022.

- [15] D.A. Anderson, R.E. Sapiro, L.F. Gonçalves, R. Cardman, and G. Raithel, "Optical Radio-Frequency Phase Measurement With an Internal-State Rydberg Atom Interferometer," *Phys. Rev. Appl.*, vol. 17, pp. 044020, Apr 2022.
- [16] Matthew T. Simons, Abdulaziz H. Haddab, Joshua A. Gordon, David Novotny, and Christopher L. Holloway, "Embedding a Rydberg Atom-Based Sensor Into an Antenna for Phase and Amplitude Detection of Radio-Frequency Fields and Modulated Signals," *IEEE Access*, vol. 7, pp. 164975–164985, 2019.
- [17] Mingyong Jing, Ying Hu, Jie Ma, Hao Zhang, Linjie Zhang, Liantuan Xiao, and Suotang Jia, "Atomic superheterodyne receiver based on microwave-dressed Rydberg spectroscopy," *Nature Physics*, vol. 16, no. 9, pp. 911–915, Sep 2020.
- [18] Vladimir Aksyuk, Christopher L. Holloway, and Matt Simons, "PHOTONIC RYDBERG ATOM RADIO FREQUENCY RECEIVER AND MEASURING A RADIO FREQUENCY ELECTRIC FIELD," U.S. Patent 20220390496-A1, Dec. 2022.
- [19] Vladimir Aksyuk, Christopher L. Holloway, and Matt Simons, "ATOMIC VAPOR CELL AND MAKING AN ATOMIC VAPOR CELL," U.S. Patent 20220018914-A1, Jan. 2022.
- [20] Nikunj Kumar Prajapati, Andrew P. Rotunno, Samuel Berweger, Matthew T. Simons, Alexandra B. Artusio-Glimpse, Stephen D. Voran, and Christopher L. Holloway, "TV and video game streaming with a quantum receiver: A study on a Rydberg atom-based receiver's bandwidth and reception clarity," *AVS Quantum Science*, vol. 4, no. 3, pp. 035001, 2022.
- [21] Peter Vouras, Kumar Vijay Mishra, and Alexandra Artusio-Glimpse, "Phase Retrieval for Rydberg Quantum Arrays," *arXiv*, 2023.